The Self-Assembly of Metaboric Acid Molecules into Bowls, Balls and Sheets

M. Elango and V. Subramanian*

Chemical Laboratory, Central Leather Research Institute, Council of Scientific and Industrial Research, Adyar, Chennai, India 600 020

N. Sathyamurthy*,†

Indian Institute of Science Education and Research (IISER) Mohali, Sector 26, Chandigarh, India 160 019

Received: March 5, 2008; Revised Manuscript Received: June 17, 2008

The structural motifs responsible for the formation of bowls, balls and sheets of orthoboric acid were pointed out in an earlier publication (Elango et al. *J. Phys. Chem. A* **2005**, *109*, 8587). It is shown in the present study that metaboric acid forms similar bowls, balls and sheets, despite the fact that the basic unit for cluster formation is different.

1. Introduction

Design and development of self-assembled nanostructures is an active area of contemporary research. Numerous studies have been made on this subject with a view to understand the relationship between the structure of the participating molecules and the structure and properties of the self-assembled supramolecule.[1−4] Earlier studies on orthorboric acid clusters had suggested the possibility of formation of bowls, balls and sheets.[5,6] It became clear that the pentagonal motif was responsible for the formation of bowl and ball structures, whereas the hexagonal motif led to the formation of sheets as long as pentagons were not included.

The term boric acid normally includes orthoboric (H_3BO_3), metaboric (HBO_2) and tetraboric ($H_4B_4O_7$) acids. When heated above 170 °C, orthoboric acid dehydrates to form metaboric acid. One of the modifications of metaboric acid (MBA), called orthorhombic metaboric acid ($H_3B_3O_6$) resembles orthoboric acid (OBA) as illustrated in Figure 1. In both the moieties, boron atom is at the center of a trigonal plane of BO_3 group. The sheet structure of MBA has been reported by Tazaki,[7] and Peters and Milberg,[8] and Coulson.[9] Zachariasen[10] reported the crystal structure of OBA. The BO_3 groups are arranged in pseudohexagonal stacked layers, which are 3.181 Å apart in OBA and 3.128 Å apart in MBA. Within each layer, the functional groups are connected to each other by hydrogen bonds.

Because of the structural similarities between meta- and orthoboric acid, it is expected that MBA can also form bowls and balls, in addition to the sheet structure. Hence it is worth exploring the possibility of formation of MBA based bowls and balls. With a view to understand the various factors governing the structure and stability of these structural motifs, electronic structure calculations have been carried out on hydrogen bonded clusters of $(MBA)_n$, $n = 2-6$, 8, 10, 12, 15 and 20.

2. Computational Details

Geometries of various clusters, $(MBA)_n$, $n = 2$-6, 8, 10, 12, 15 and 20, have been optimized without geometrical constraints at the HF/6-31G* level of theory using the G98W and G03[11,12] suite of programs. All these structure are found to be stable relative to the separated monomers. For clusters up to $n = 6$, B3LYP/6-31G* calculations were also carried out to verify the results obtained from HF/6-31G* calculations. The stabilization energies (SE) of all the clusters have been calculated using the supermolecule approach

$$\mathrm{SE} = -\left(E_{\mathrm{cluster}} - \sum_{i=1}^{n} E_i\right) \quad (1)$$

where n is the total number of monomers and E_{cluster} and E_i refer to the energies of the cluster and the monomer, respectively. The results have been corrected for basis set superposition error (BSSE) following the procedure adopted by Boys and

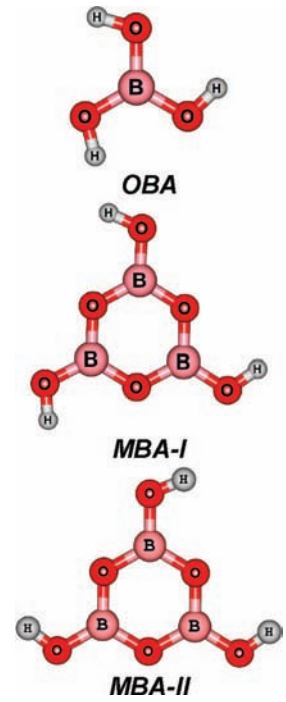

Figure 1. Optimized geometries of ortho- and metaboric acid molecules obtained from B3LYP/6-31G* calculations.

* Authors for correspondence. V.S.: e-mail, subuchem@hotmail.com; tel, +91 44 24411630; fax, +91 44 24911589. N.S.: e-mail, nsath@iitk.ac.in; tel, +91-172-2790188; fax, +91-172-2790188.

† Honorary Professor, Jawaharlal Nehru Centre for Advanced Scientific Research, Bangalore 560 064, India.

10.1021/jp8019254 CCC: $40.75
Published on Web 08/12/2008

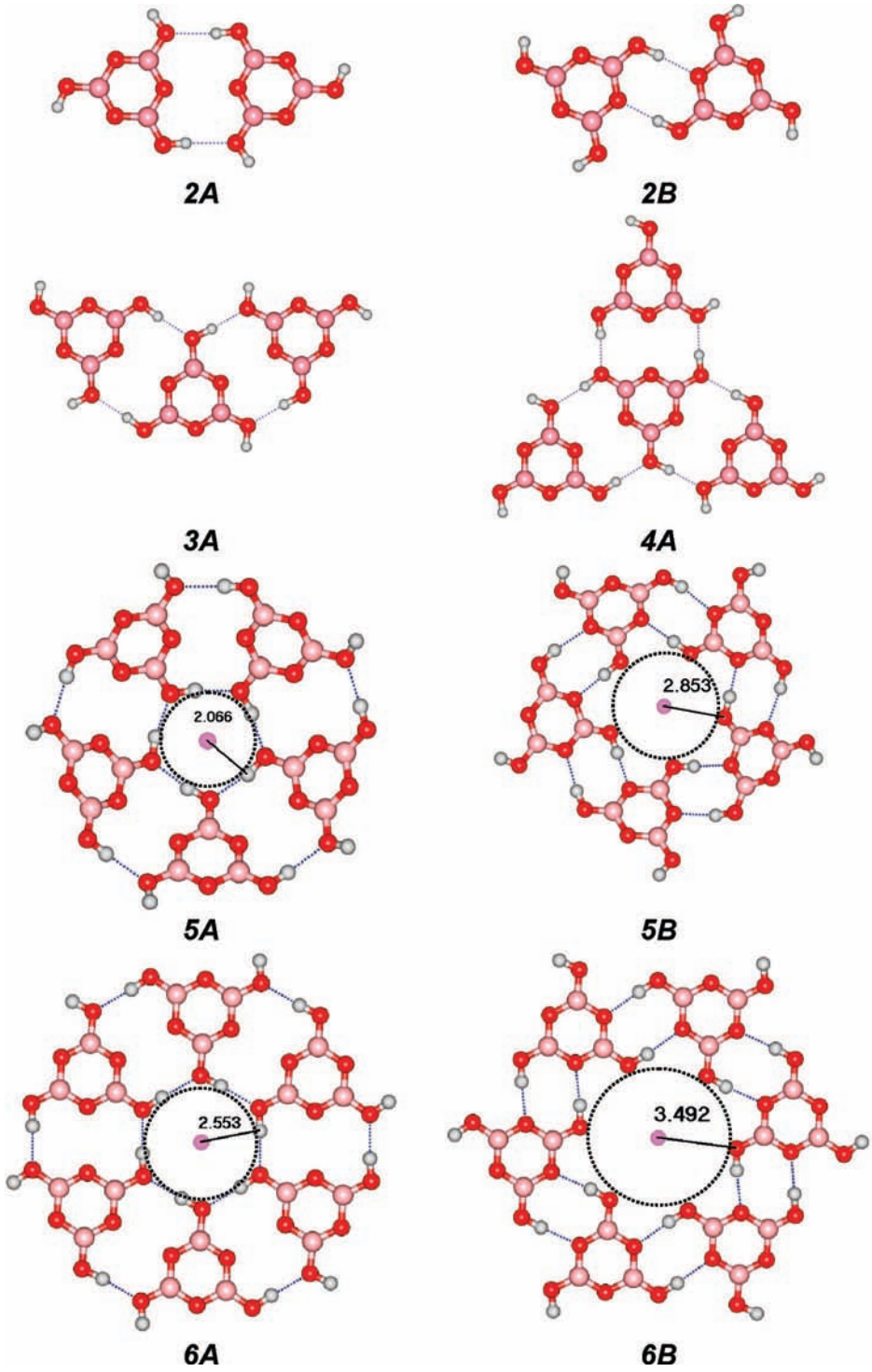

Figure 2. Optimized structures of metaboric acid clusters, $(MBA)_n$, where $n = 2-6$ obtained using B3LYP/6-31G* level of calculation. The black dotted circle is the central H-bonded cavity and the radius of the circle is given in Å.

Bernardi.[13] Vibrational frequencies were calculated for $(MBA)_n$, $n = 1-6$. They were scaled[14] by a factor of 0.8929 for comparison with the available experimental results. Calculated frequencies for the clusters clearly indicate that they are true minima on the potential energy surface. The theory of atoms-in-molecules (AIM) has been used to characterize the hydrogen bonding and other nonbonding interactions between monomers using topological properties of electron density at the bond critical points (BCPs) using the AIM2000 package.[15] In addition, molecular electrostatic potential (MESP) maps[16] of various clusters have been generated using GaussView 3.0 software package.[17]

3. Results and Discussion

Structure and Stability. The equilibrium geometry of MBA is planar. It can exist as two conformers, MBA-I and MBA-II, as illustrated in Figure 1. B3LYP and HF calculations show that MBA-I is more stable than MBA-II by 1 kcal/mol. Therefore, clusters of MBA-I have been investigated in the present study. For brevity, MBA-I is referred to as MBA in the remaining part of the text. The average B−O bond distance in the six-membered, boron−oxygen ring is 1.373 Å, while the average out-of-ring B−O bond distance is 1.349 Å. The respective calculated B−O length from B3LYP (HF) method

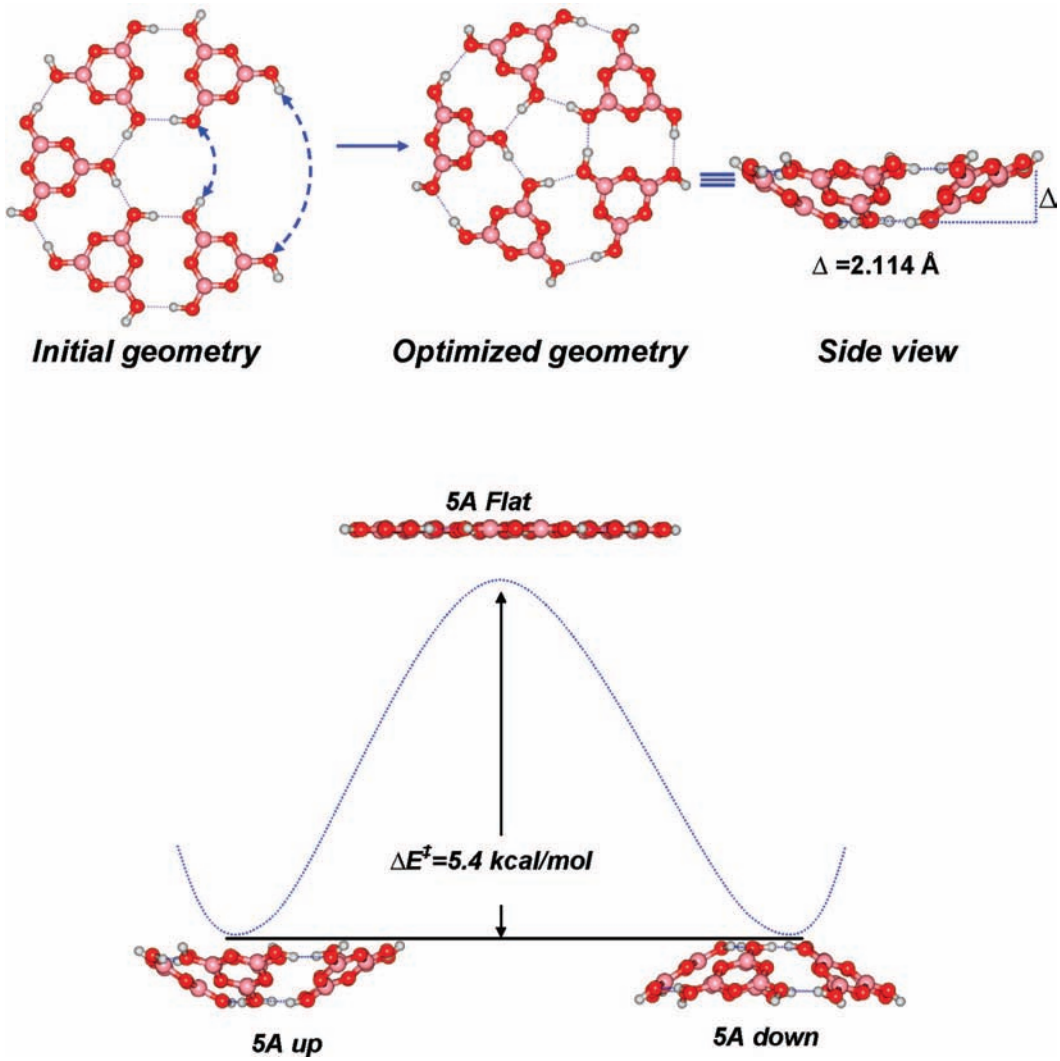

Figure 3. Geometrical features of cyclic pentamer **5A** calculated using B3LYP/6-31G* level of theory. The bowl depth is represented as Δ.

TABLE 1: Hydrogen Bonding Interaction Distances and Angles for $(MBA)_n$ Clusters, Where $n = 1-6$, 20, Obtained Using B3LYP/6-31G* Calculations

	H-bonding type	O−H (Å)	(O)H···O (Å)	O−H···O (deg)
1		0.968	–	–
2A		0.978	1.935	176.6
2B		0.978	1.894	177.2
3A		0.980	1.900	176.0
4A		0.981	1.894	176.0
5A	inner OH···O	0.988	1.793	166.8
	outer OH···O	0.978	1.978	167.5
5B	inner OH···O	0.976	1.894	163.8
	outer OH···O	0.976	2.000	164.8
6A	inner OH···O	0.986	1.882	177.0
	outer OH···O	0.979	1.895	176.2
6B	inner OH···O	0.978	1.903	174.7
	outer OH···O	0.977	1.888	176.9
20A[a]		0.957	2.005	162.6

[a] Obtained from HF/6-31G* calculation.

is 1.381 Å (1.367 Å) and 1.357 Å (1.343 Å). The average O−H length obtained from B3LYP and HF calculations are 0.968 Å and 0.947 Å, respectively. The average O−H distance obtained from crystal structure is 0.87 Å. All the calculated values are in close agreement with the values obtained from crystal structure.[7−9]

Figure 2 illustrates the optimized geometrical structures of $(MBA)_n$ clusters (where $n = 2-6$). Two different hydrogen bonded dimers are possible as shown in **2A** and **2B**. The two different types of hydrogen bonding pattern in these two structures are designated as **A-type** and **B-type**, respectively.

TABLE 2: Stabilization Energies (SE) in kcal/mol of Metaboric Acid Clusters Obtained from HF/6-31G* and B3LYP/6-31G* Calculations

	BSSE					
	uncorrected		corrected		BSSE + ZPE corrected	SE per MBA
	HF	B3LYP	HF	B3LYP	HF	HF
2A	9.2	11.9	8.0	9.9	7.0	4.0
2B	8.2	11.1	7.2	9.7	6.4	3.6
3A	19.1	24.9	16.5	20.6	14.5	5.5
4A	29.3	38.8	25.2	32.0	22.1	6.3
5A	47.2	63.6	40.8	53.5	35.8	8.2
5B	37.4	51.4	33.6	41.3	30.6	6.7
6A	60.1	78.8	51.2	64.3	45.1	8.5
6B	49.7	67.3	43.8	58.3	39.7	7.3
6A-I	57.7	–	49.9	–	–	8.3
8A	86.9	–	75.3	–	–	9.4
10A	117.0	–	101.0	–	–	10.1
12A	147.2	–	128.0	–	–	10.6
15A	197.0	–	172.0	–	–	11.5
20A	302.4	–	1037.0	–	–	51.9
20A-sheet	249.8	–	211.0	–	–	10.6
20-sheet[a]	258.7	–	227.0	–	–	11.4

[a] As predicted in ref 8.

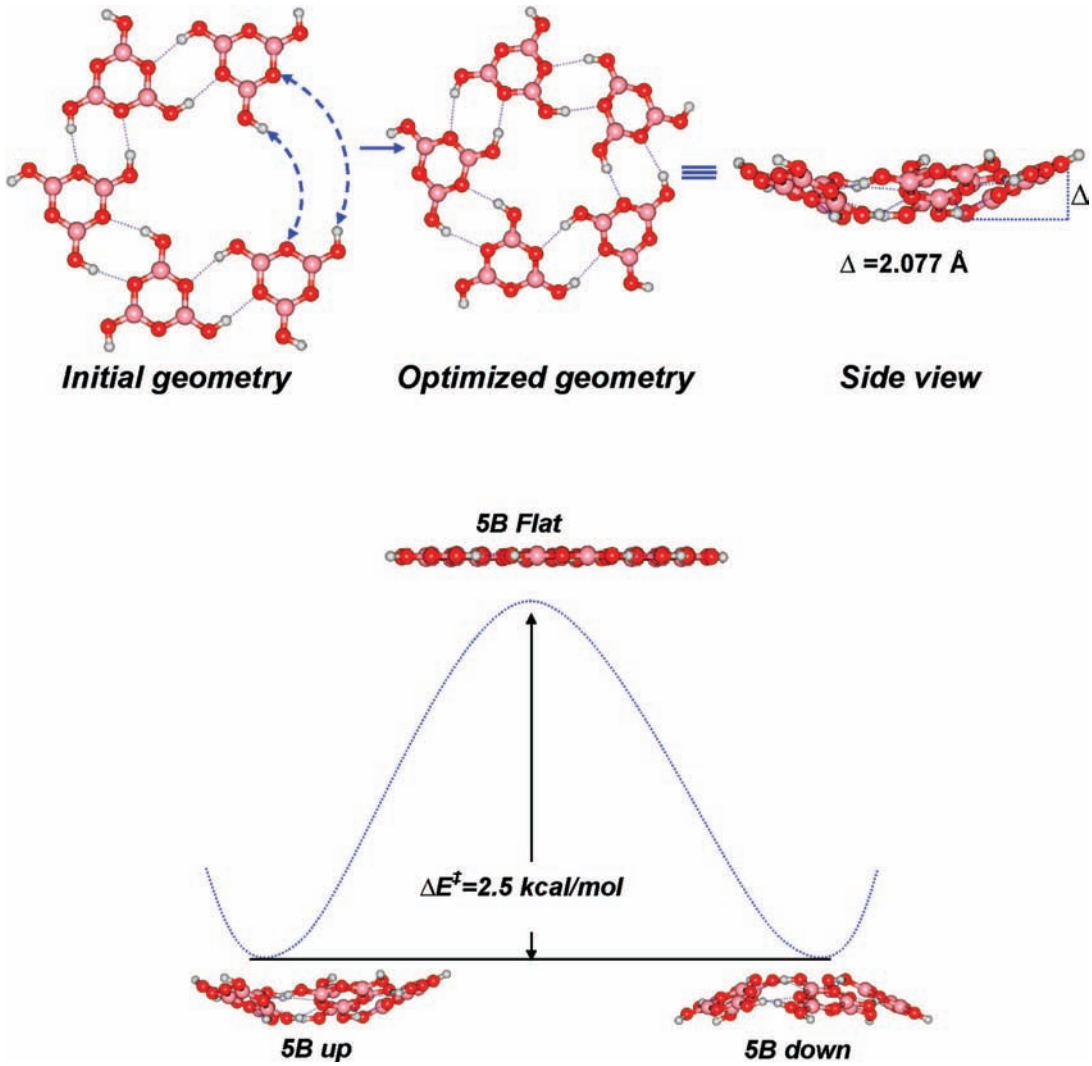

Figure 4. Geometrical features of cyclic pentamer **5B** calculated using B3LYP/6-31G* level of theory. The bowl depth is represented as Δ.

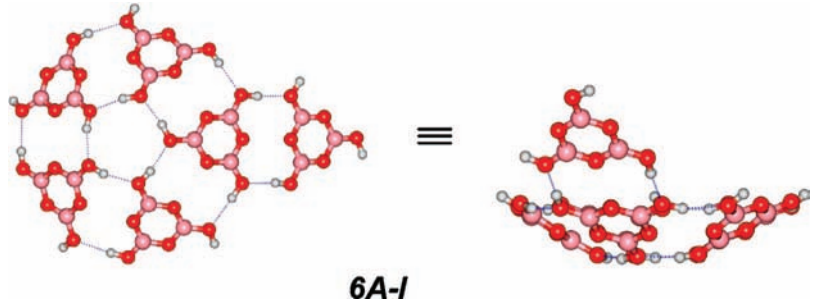

Figure 5. Optimized structure of **5A** based cluster, **6A-I**, obtained using the HF/6-31G* level of calculation.

In these dimers, the two MBA molecules act as H donors as well as acceptors. As a result, it is possible to observe two O−H···O bonds with identical geometrical parameters. Hydrogen bonding geometries for the $(MBA)_n$ clusters, where $n = 1-6$ and 20 are listed in Table 1. The hydrogen bonding distances obtained from HF and B3LYP calculations are in good agreement with that of the experimental values.[7−9] The calculated O−H···O bond length and hydrogen bond angle are 1.934 Å and 176.6°, respectively, for **2A**. The corresponding values for **2B** are 1.894 Å and 177.2°. The stabilization energies for $(MBA)_n$ clusters, where $n = 2-6$, 8, 10, 12, 15 and 20, are listed in Table 2. For clusters up to $n = 6$, the zero point energy (ZPE) corrected SEs are also included. The SE of **2A** calculated at HF/6-31G* and B3LYP/6-31G* levels of theory is 8.0 and 9.9 kcal/mol, respectively. The corresponding SE values for **2B** are 7.2 and 9.7 kcal/mol. It is interesting to note that SE of **2A** is greater than that of **2B**.

3A is a hydrogen bonded planar structure in which the central MBA is hydrogen bonded to two MBAs on both sides. HF/6-31G* and B3LYP/6-31G* calculations yield SE values of 16.5 and 20.6 kcal/mol, respectively. In the structure **4A** the central MBA is hydrogen bonded to other MBAs in a symmetric fashion to form a triangular motif. This type of hydrogen bonding interaction is observed in MBA sheets,[7−9] akin to the covalent bonding in graphene sheets.

Interestingly, optimized geometries of cyclic MBA pentamers, **5A** and **5B**, adopt (nonplanar) bowl shapes. The structural features of these bowls obtained from B3LYP calculation are

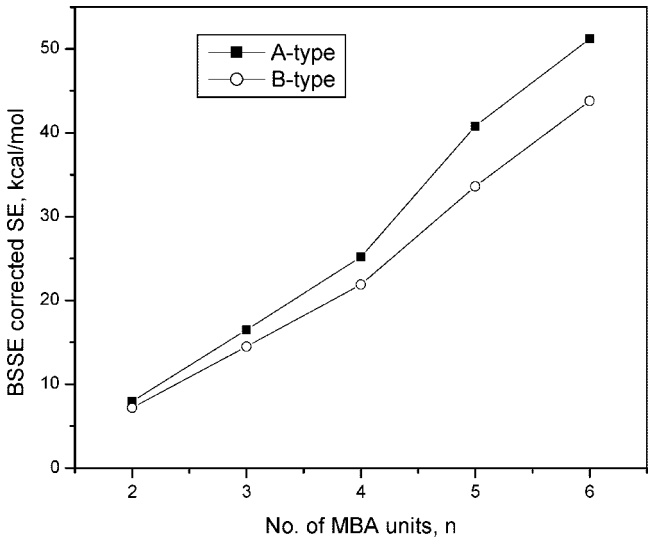

Figure 6. The variation of SE values with the number of MBA units with A-type and B-type interactions.

illustrated in Figure 3 and Figure 4. The calculated bowl depths for **5A** and **5B** are 2.114 and 2.077 Å, respectively. These bowls can undergo inversion, and the corresponding inversion barriers are 5.4 and 2.5 kcal/mol, respectively. This also implies that the planar structure (**5A-flat** and **5B-flat**) is not stable; it is the transition state between the two bowls (**5A-up/5A-down** and **5B-up/5B-down**). There are two different hydrogen bonding distances in **5A** and **5B**, with the inner O−H···O distance (1.785 for **5A** and 1.871 Å for **5B**) being considerably shorter than the outer O−H···O distance (1.986 for **5A** and 1.993 Å for **5B**). All the inner hydrogen bonds are identical, and the same is true for all the outer hydrogen bonds.

TABLE 3: Calculated[a] Vibrational Frequencies of Various (MBA)$_n$ Clusters, Where $n = 1-6$, at HF/6-31G* Level, Along with Computed Red Shifts in the O−H Stretching Mode

		scaled frequencies (cm^{-1})		red shift (cm^{-1})	
		ss	as	ss	as
1		3688	3689	–	–
2A		3596	3601	92	86
3A		3583	3600	106	88
4A		3561−3581	3564−3589	108−128	98−123
5A	inner	3490	3521−3545	198	143−167
5A	outer	3607	3609−3612	81	76−78
6A	inner	3513	3532−3596	176	129−155
6A	outer	3593	3558−3599	96	88−92

[a] After scaling by a factor of 0.8929.

Unlike the cyclic pentamer, the cyclic hexamers **6A** and **6B** are planar! This does not come as a surprise as the crystal structure of metaboric acid is known to be made up of layers of hydrogen bonded networks of hexagons. In these hexamer motifs, the inner and outer O−H···O hydrogen bonds have identical bond lengths and angles. A comparison of SE values for the flat hexamer (**6A**) and the bowl hexamer (**6A-I**) shows that the planar hexamer is more stable. Figure 5 presents the optimized geometry of the bowl based hexamer **6A-I**.

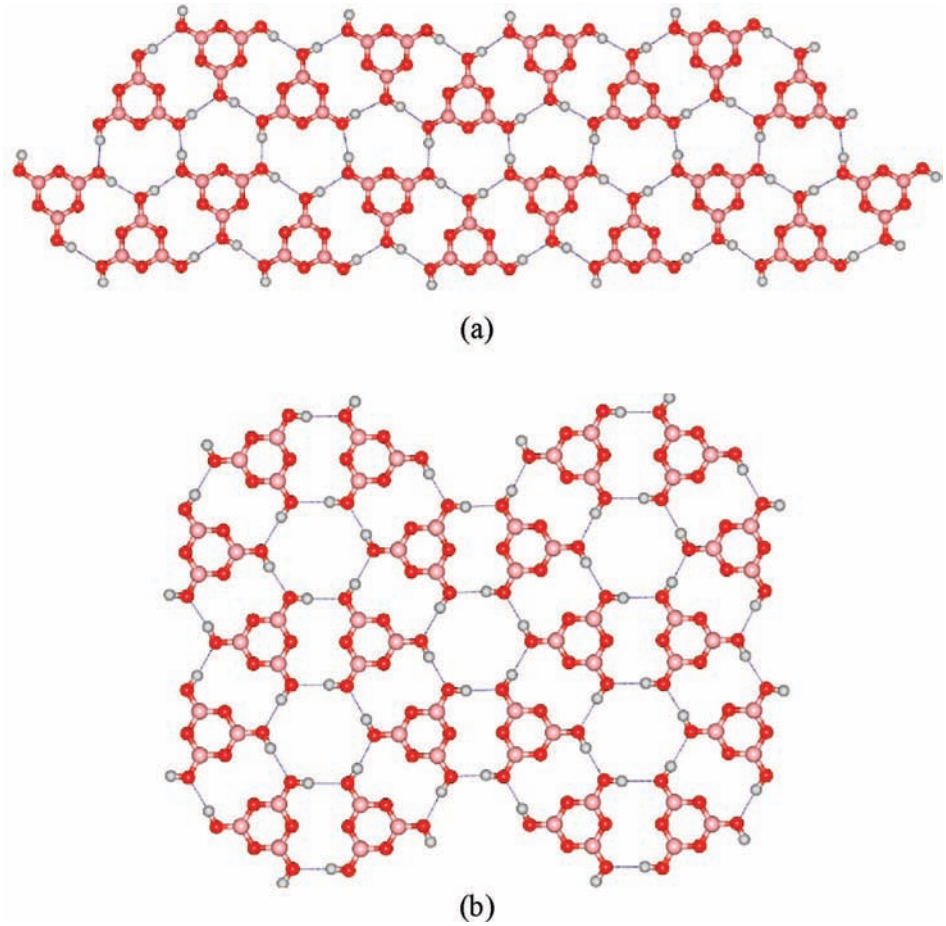

Figure 7. Model of the sheet structures formed by MBA molecules: (a) mica-like zigzag sheet structure observed in crystal structure[7−9] and (b) hexagon based sheet structure from the present study.

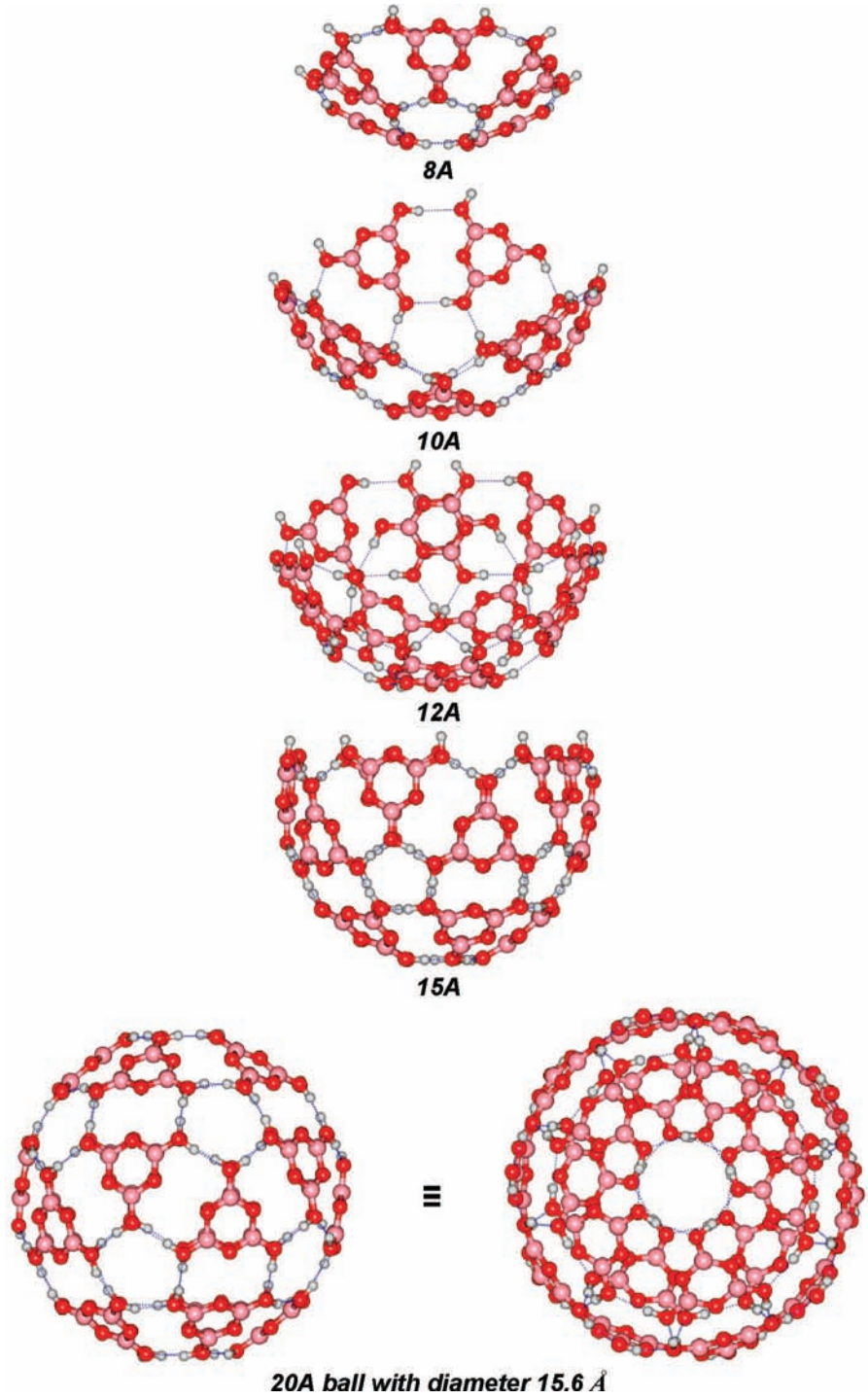

Figure 8. Optimized geometries of metaboric acid clusters, $(MBA)_n$, where $n = 8$, 10, 12, 15 and 20, obtained using the HF/6-31G* level of calculation.

It is well-known that graphite sheet is made up of hexagonal motifs. To form bowls and balls of carbon, the pentagonal motif is essential. Although a similar pentameric motif is necessary to form bowls and balls of MBA, the nature of interaction between the carbon atoms and between MBA molecules is entirely different. The bonding in carbon clusters is covalent and the resulting structure is largely rigid. The interaction between MBA moieties in $(MBA)_n$ clusters, on the other hand, is hydrogen bonding and the resulting structure is flexible.

An attempt has been made to compare the SE values of two different types of interaction observed in the MBA clusters. It is important to note from Figure 6 that the A-type interaction is more favorable than the B-type. It can be seen from the SE values that the pentamer **5A** and hexamer **6A** are more stable than **5B** and **6B** by 7.2 and 7.4 kcal/mol, respectively. The crystal structure of MBA clusters confirms that MBA sheets are stabilized by the A-type interaction. Further, the central cavity present in pentamer and hexamer of A-type is smaller than that in clusters of B-type. In the present study, A-type interaction is used for the formation of larger clusters of MBA.

The crystal structure[7−9] of MBA reveals a zigzag arrangement of MBA molecules, similar to the arrangement in mica as illustrated in Figure 7a. Therefore, the stability of the mica-like sheet and the hexagon based sheet structure containing 20

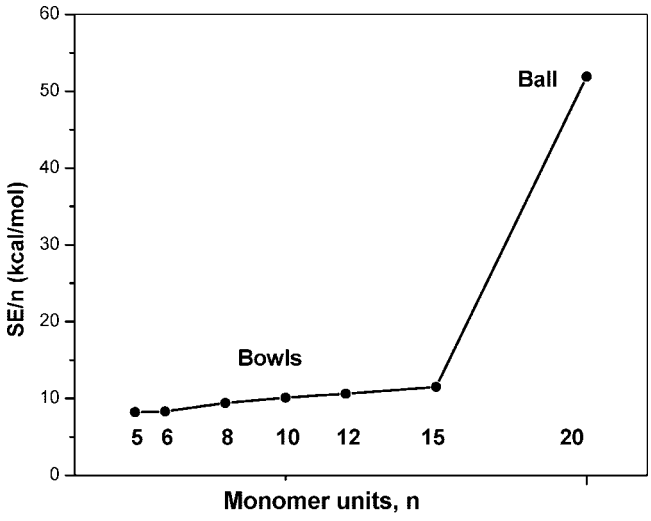

Figure 9. Variation of stabilization energy (SE) per metaboric acid molecule as a function of the size of the cluster, obtained from HF/6-31G* calculations.

TABLE 4: Electron Density and Laplacian of Electron Density at the Hydrogen Bonding Critical Points for $(MBA)_n$ Clusters, Where $n = 2-6$, 20, Using HF/6-31G* Calculations

	H-bonding type		electron density (e/a_o^3)	Laplacian of electron density (e/a_o^5)
2A			0.017	0.016
3A			0.019	0.017
4A			0.020	0.018
5A	inner	OH···O	0.024	0.021
	outer	OH···O	0.014	0.013
6A	inner	OH···O	0.019	0.017
	outer	OH···O	0.019	0.017
20A	OH···O		0.021	0.019
	O···O		0.008	0.007

monomers was investigated at the HF/6-31G* level of theory. The optimized geometries of both the sheets are shown in Figure 7. It is worth pointing out that the hexagonal sheet structure is made up of MBA whereas the mica-like sheet is made up of MBA II. The BSSE corrected stabilization energy for both the sheets given in Table 2 shows that mica-like structure is more stable than the hexagon based sheet.

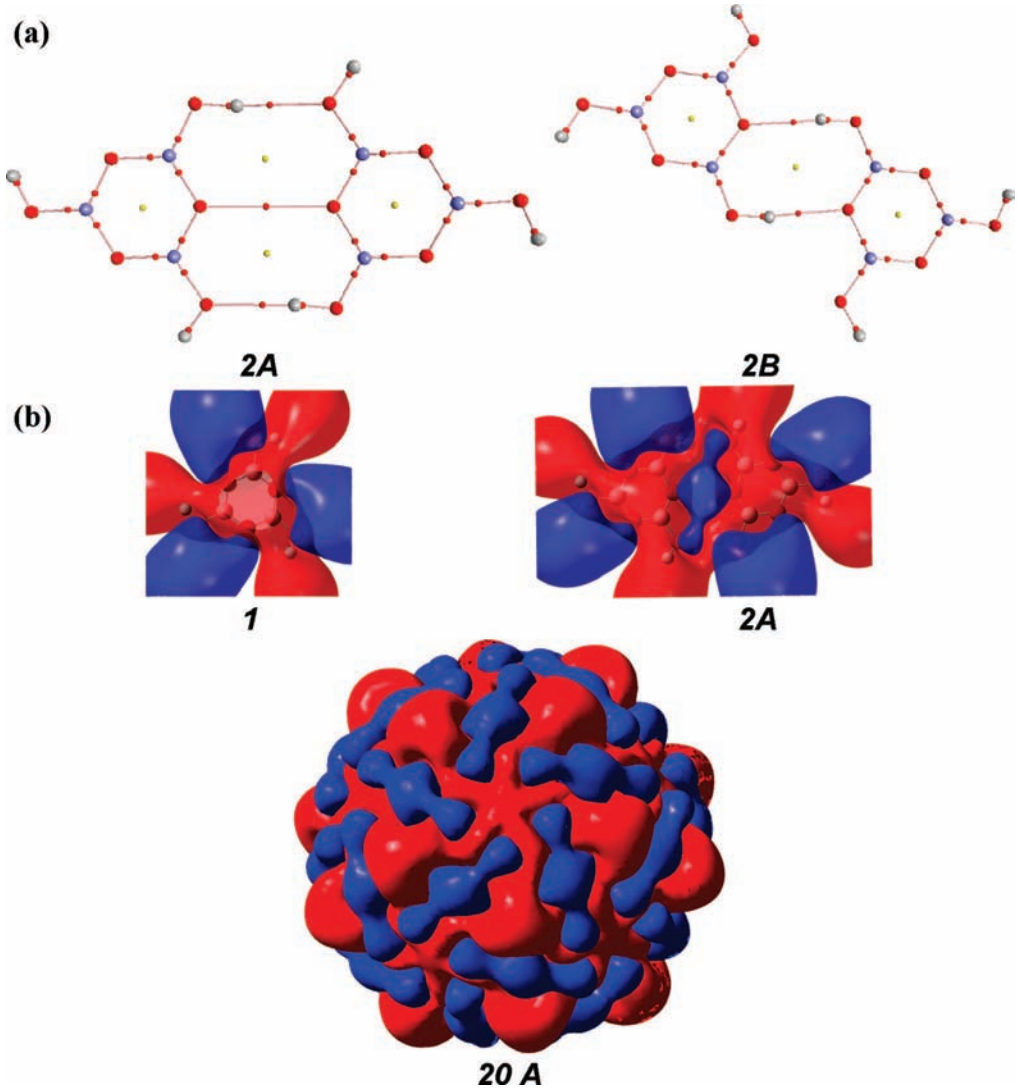

Figure 10. (a) AIM derived molecular graphs of dimers of metaboric acid, as obtained from HF/6-31G* calculations. Bond critical points are denoted by small red dots, and the yellow dots represent ring critical points. (b) Molecular electrostatic potential map (−0.005 au isosurface) of metaboric acid, dimer (**2A**) and **20A** ball calculated at HF/6-31G* level of calculation. See text for details. Negative potential is represented by blue color, and positive potential is given in red color.

Optimized geometries of larger clusters based on **5A** are shown in Figure 8. Clearly, the 8-mer (**8A**), 10-mer (**10A**), 12-mer (**12A**) and 15-mer (**15A**) are all bowl shaped. Three-fourths-fullerene topology in $(MBA)_n$ clusters emerges for $n = 15$. It is thus expected that a fullerene-like topology would be obtained with more MBA molecules self-assembled by hydrogen bonding. With the addition of another 5 molecules to the 15-mer described above, the structure becomes a full-fledged metaboric acid ball! The diameter of the ball (**20A**) as obtained from HF/6-31G* calculation is 15.597 Å. It is interesting to note that all the hydrogen bonds in **20A** are identical: the hydrogen bond length is 2.005 Å, and the angle is 162.6°. To assess the stability of large MBA clusters, SE values of the clusters are plotted against the size of the cluster. It is important to point out that the SE per MBA moiety increases with increase in the size of the bowl as shown in Figure 9. As the bowls grow into a ball, the SE increases drastically, thus indicating that the formation of **20A** and other ball structures is energetically favorable.

Frequency. Symmetric and asymmetric O−H stretching frequencies for MBA and its clusters up to $n = 6$ as computed by the HF/6-31G* method and scaled by a factor of 0.8929 are reported in Table 4. The computed values for MBA are 3688 (ss) and 3689 cm^{-1} (as), and the experimental values are 3257 and 3356 cm^{-1}, respectively.[18] The O−H stretching frequencies for dimer **2A** are 3596 and 3601 cm^{-1}, and the calculated red shifts are 92 and 86 cm^{-1}, respectively, thus indicating hydrogen bond formation. The computed red shifts in the range 88−128 cm^{-1} for the **3A** and **4A** reiterate the characteristics of hydrogen bonding. Due to slightly different geometrical parameters obtained for inner and outer peripheries of pentamer as well as hexamer, the red shifts are also different. Hydrogen bonding in the inner periphery results in larger red shifts than in the outer periphery for both **5A** and **6A**.

Atoms in Molecules. The AIM theory has been used to characterize the hydrogen bonding and other nonbonding interactions in $(MBA)_n$, $n = 2 - 6$ and 20, and the resulting parameters are listed in Table 3. The values of electron density at the hydrogen bond critical points (CPs) fall in the range 0.017−0.024 e/a_o^3. The Laplacian of the electron density at the CPs provide valuable information on electron density accumulation or depletion. The calculated values (0.013−0.021 e/a_o^5) of the Laplacian for the hydrogen bonds are all positive, indicating the depletion of electron density at the hydrogen bond CPs. Figure 10a illustrates the AIM topology of $(MBA)_2$.

Molecular Electrostatic Potential. Since molecular electrostatic potential (MESP) map is a valuable tool to understand the reactivity, it has been computed for **MBA**, **2A** and **20A** and the −0.005 au isosurfaces are included in Figure 10. It can be seen that the MESP minimum occurs at the position of the lone pairs of the oxygen atom. These regions provide possible anchoring sites for further hydrogen bonding. It is to be noted in the case of **20A** that the negative valued MESP features are seen only at the outside of the ball, while the positive MESP values are observed both inside and outside of the ball. This is very similar to what is observed for C_{60}.[19] Inside the cage MESP is positive everywhere, and outside there are regions of negative and positive potentials. Therefore, it is possible to host negatively charged species inside the **20A** ball.

It is worth comparing the self-assembled structures of ortho- and metaboric acid clusters. The equilibrium geometry of both molecules is planar, and they exhibit C_{3h} symmetry. It can be seen from our previous studies on boric acid clusters that self-assembled motifs are made up of one type of O−H···O hydrogen bonding interaction. In the case of metaboric acid, two kinds of O−H···O interactions are possible as shown in Figure 2, structures **2A** and **2B**. Although both molecules form nonplanar cyclic pentamers, their geometrical parameters such as bowl depth and inversion barrier are different. The pentamers prefer to adopt nonplanar bowl structures on further addition of boric acid/metaboric acid molecules. In both cases, the nonplanar pentamer is the crucial precursor for the hydrogen bonded self-assembled ball shaped structures. Similarly, hydrogen bonded hexamers adopt a planar sheet like structure akin to that of graphene. This sheet structure continues to be planar as long as a pentamer motif is not included. Interestingly, the mica-like sheet structure is more stable than the hexagon based structure for the 20-mer of MBA. It is important to emphasize that both the molecules self-assemble in a similar fashion to give rise to bowls, balls and sheet structures. It can also be seen that the electrostatic potential maps of orthoboric and metaboric acid balls are similar. Hence, their reactivity and host−guest interactions are also expected to be similar.

4. Summary and Conclusion

In summary, *ab initio* quantum chemical calculations suggest that metaboric acid molecules can self-assemble into various shapes like bowls and balls as long as they are built around $(MBA)_5$ moieties. The planar hexamer based structures, on the other hand, continue to be planar as long as a pentagonal motif is not introduced. Metaboric acid ball **20A** is predicted to be highly stable. Therefore, energetically it would be more favorable to build bowls and balls of MBA clusters from $(MBA)_5$ units and not $(MBA)_6$!

Acknowledgment. The authors are grateful to the Council of Scientific and Industrial Research (CSIR), New Delhi, India, for its financial support. N.S. thanks the Department of Science and Technology, New Delhi, for a J. C. Bose Fellowship. M.E. thanks CSIR for a Senior Research Fellowship.

References and Notes

(1) Lehn, J.-M. (Nobel lecture) *Angew. Chem., Int. Ed.* **1988**, *27*, 89.
(2) Lehn, J.-M. *Supramolecular chemistry, concepts and perspectives*; VCH: Weinheim, 1995.
(3) Atwood, J. L.; Steed, J. W. *Encyclopedia of Supramolecular Chemistry*; CRC Press: Boca Raton, FL, 2004.
(4) Desiraju, G. R. *Angew. Chem., Int. Ed.* **2007**, *46*, 8342.
(5) Elango, M.; Parthasarathi, R.; Subramanian, V.; Sathyamurthy, N. *J. Phys. Chem. A* **2005**, *109*, 8587.
(6) (a) Wang, W.; Zhang, Y.; Huang, K. *J. Phys. Chem. B* **2005**, *109*, 8562. (b) Wang, W.; Zhang, Y.; Huang, K. *Chem. Phys. Lett.* **2005**, *405*, 425.
(7) Tazaki, H. *J. Sci. Hiroshima Univ.* **1940**, *A10*, 37; *J. Sci. Hiroshima Univ.* **1940**, *A10*, 55.
(8) Peters, C. R.; Milberg, M. E. *Acta Crystallogr.* **1964**, *17*, 229.
(9) Coulson, C. A. *Acta Crystallogr.* **1964**, *17*, 1086.
(10) Zachariasen, W. H. *Z. Kristallogr.* **1934**, *88*, 150; *Acta Crystallogr.* **1954**, *7*, 305.
(11) Frisch, M. J.; et al. *Gaussian 98*, revision A.7; Gaussian, Inc.: Pittsburgh, PA, 1998.
(12) Frisch, M. J.; et al. *Gaussian 03*, revision A.1; Gaussian, Inc.: Pittsburgh, PA, 2003.
(13) Boys, S. F.; Bernardi, F. *Mol. Phys.* **1970**, *19*, 553.
(14) Scott, A. P.; Radom, L. *J. Phys. Chem.* **1996**, *100*, 16502−16513. Fogarasi, G.; Pulay, P. *Annu. Rev. Phys. Chem.* **1984**, *35*, 191.
(15) Bader, R. F. W. *Atoms in Molecules: A Quantum Theory*; Clarendon Press: Oxford, U. K., 1990. Biegler-Konig, F.; Schonbohm, J.; Derdau, R.; Bayles, D.; Bader, R. F. W. *AIM 2000*, version 1; Bielefeld, Germany, 2000. Parthasarathi, R.; Subramanian, V.; Sathyamurthy, N. J. *Phys.Chem. A* **2005**, *109*, 843. Parthasarathi, R.; Subramanian, V. In *Hydrogen Bonding-New Insight, Challenges and Advances in Computational Chemistry and Physics Series*; Grabowski, S. J., Ed.; Kluwer: New York, 2006; p 1. Grabowski, S. J.; Sokalski, W. A.; Dyguda, E.; Leszczynski, J. *J. Phys. Chem. B* **2006**, *110*, 6444. Parthasarathi, R.; Subramanian, V.; Sathyamurthy, N. *J. Phys. Chem. A* **2006**, *110*, 3349. Parthasarathi, R.; Subramanian, V.; Sathyamurthy,

N.; Leszczynski, J. *J. Phys. Chem. A* **2007**, *111*, 2. Parthasarathi, R.; Subramanian, V.; Sathyamurthy, N. *J. Phys. Chem. A* **2007**, *111*, 13287.

(16) Gadre, S. R.; Shirsat, R. N. *Electrostatics of Atoms and Molecules*; Universities Press: Hyderabad, India, 2000. Tomasi, J.; Mennucci, B.; Cammy, M. *Molecular Electrostatic Potentials: Concepts and Applications*; Murray, J. S., Sen, K. D., Eds.; Elsevier: Amsterdam, 1996.

(17) *GaussView 3.0*; Gaussian Inc.: Pittsburgh, PA, 2003.

(18) Parsons, J. L. *J. Chem. Phys.* **1960**, *33*, 1860.

(19) Jemmis, E. D.; Subramanian, G.; Sastry, G. N.; Mehta, G.; Shirsat, R. N.; Gadre, S. R. *J. Chem. Soc., Perkin Trans.* **1996**, *2*, 2343.

JP8019254